International Journal of Electrospun Nanofibers &Applications
Vol. 7 no. 1 (June, 2021)

Received: 02nd January 2021 *Revised: 25th March 2021* *Accepted: 23rd May 2021*

Electrospun Polyethylene Oxide-Hectorite Clay Composite Nanofibers

Sudha Madhugiri, John. P. Ferraris, Kenneth J. Balkus Jr.*

Department of Chemistry and the UTD Nanotech Institute
University of Texas at Dallas, Richardson, TX-75083-0688, USA.

Abstract: *Nanocomposite fibers with an average diameter of 200 nm were electrospun from a colloidal suspension of polyethyleneoxide (PEO) /hectorite clay. The increase in the interlamellar spacing of the clay, as shown by XRD, is consistent with intercalation of PEO between the hectorite layers. In the presence of clay the fibers form spider web-like structures not observed with pure PEO. The fibers were further characterized by SEM, DSC and FTIR spectroscopy.*

Keywords: *nanofibers, electrospinning, hectorite, polyethylene oxide*

1. INTRODUCTION

Polymer-layered silicate nanocomposites have received a great deal of attention in the past decade [1-10]. The optimum blending of polymers and layered materials can lead to nanocomposites with greater tensile properties, and heat resistance than the pure materials. It has been shown that polymer-layered nanosilicates exhibit increased modulus, impact strength and heat distortion temperatures [1-3]. Composites of the conducting polymer polypyrrole and the clay montmorillonite exhibit higher conductivites [4]. Composites of electroluminescent poly[2-methoxy-5-(2'-ethyl-hexyloxy)-1,4-phenylenevinylene] (MEH-PPV)–and organo clay exhibit higher quantum efficiencies for light emitting diodes [5]. Composites of polyethylene oxide (PEO) and Gd^{3+}-hectorite have been studied as oral MRI contrast agents [6-7]. The d-spacing between the layers in these clay materials can be increased by intercalating polymers and/or by ion exchanging [6-12]. The resulting composites have been studied for their change in various properties including mechanical behavior. In an effort to produce well dispersed nanocomposites, nylon 6-montmorillonite composites have been electrospun to form nanofibers with aligned montmorillonite layers and nylon crystallites [13]. The application of these composites often depends on the ability to process them in different configurations such as films and fibers.

Electrospinning is a technique that can be used to produce high surface area nanofibers under the influence of electrostatic field [14-19] and many polymers including polyethylene oxide (PEO) have been successfully electrospun using this technique [15-18, 20] Along with the ability to form nanofibers, PEO has been shown to readily intercalate in between

* corresponding author: E-mail: *balkus@utdallas.edu*

the layers of aluminosilicate clays [6,8, 21-22]. We have now combined these two features to produce high surface area PEO/clay nanocomposite fibers.

The clay employed in this study is hectorite having the formula $R_{0.33}^{+}(Mg_{2.67}Li_{0.33})Si_4O_{10}(OH)_2$ ($R = Al^{3+}$) shown in figure 1b. The structure of the hectorite consists of a corner linked tetrahedral sheet and an edge linked octahedral sheet in ~2:1 ratio where Si^{4+} (substituted by Al^{3+} frequently) is bonded to four oxygens in a tetrahedron. The octahedral layer contains the charge balancing and exchangeable cations such as Li^{+} or Mg^{2+}. Among the clay materials, the Smectite type layered aluminosilicates such as hectorite, tend to be employed for composites more often than others 8-10,21-22]. This is largely because of their ability to expand or contract the layers while maintaining a crystalline structure [23]. The intercalation of polymers such as polyethylene oxide (PEO) between the clay layers, as shown schematically in figure 1b is known to increase the interlayer d-spacing [6, 9, 21-22].

The present strategy for fabrication of nanocomposite fibers is to first prepare polymer/clay nanocomposites by intercalating PEO between the layers of hectorite and then, to electrospin the resulting composite. Clay materials, which are hydrophilic, tend to phase separate in polymer solutions prepared in organic solvents [5]. In contrast, water-soluble PEO is expected to readily intercalate between the clay layers and remain intact during electrospinning. The intercalation of PEO depends on the length of the

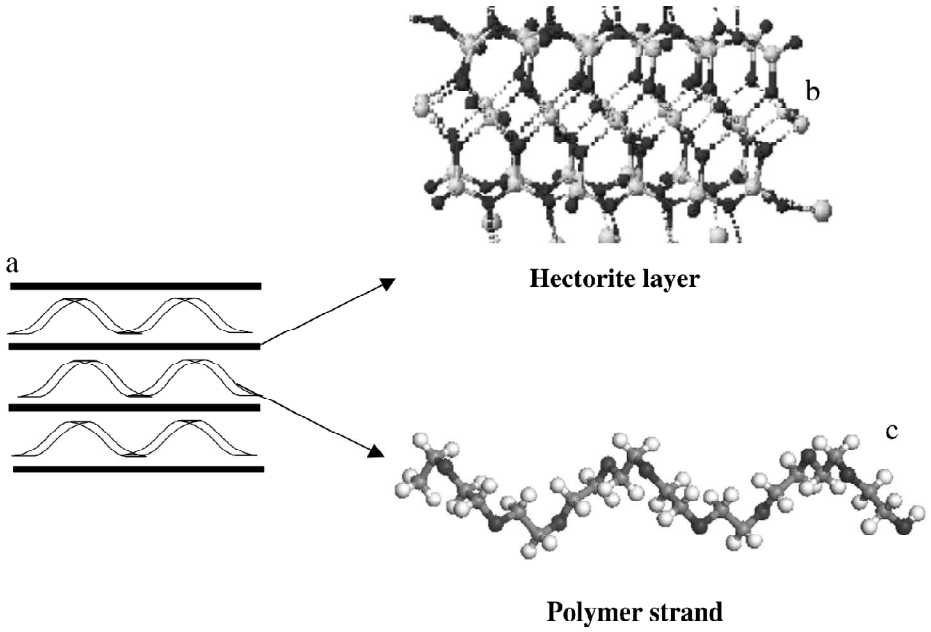

Figure 1: (a) Schematic representation of the intercalation of PEO between hectorite layers, (b) the structure of hectorite calculated using CACHE from the crystallographic parameters in reference 7, (c) PEO strand showing 10 monomer units calculated using Material Studio

polymer chains [8] and in the present study it was observed that PEO with high molecular weights (e.g. $5x10^6$ g/mol) phase separated from the clay. Molecular weight becomes an even more important variable in this case because one needs a homogenous dispersion of PEO and clay with a viscosity suitable for electrospinning. Finally, the amount of clay that can be uniformly dispersed without phase separation must be balanced with these other variables in forming a precursor gel.

2. EXPERIMENTAL SECTION

Electrospinning is a useful technique for producing nanofibers of various polymers including PEO [16-20]. In our process a 3 mL syringe barrel is charged with a viscous PEO gel which forms a droplet at the end of the syringe needle which produces a fine polymer jet when an electric current is applied. The jet starts to divide into fibrils with like charge, which repel each other forming a mesh. This process also leads to the evaporation of the solvent and the forming fibers migrate to a target attached to the oppositely charged electrode [16].

Solutions for electrospinning PEO/hectorite composite fibers were prepared using PEO (Aldrich) with molecular weights of $2x10^5$, 10^6 and $5x10^6$ g/mol. Natural hectorite was purchased from Clay Minerals Repository, Columbia, Missouri. The natural hectorite contained $CaCO_3$ impurities, which were removed using 2M HCl. The carbonate-free clay was thoroughly washed with water and centrifuged to obtain a free flowing powder. The resulting sample of hectorite was pulverized using a wig-l-bug to reduce the particle size to 1.5-2 μm for better dispersion in the PEO solutions.

A range of concentrations using the different molecular weights of PEO were explored to prepare aqueous solutions of PEO. Once the desired viscosity of the solution was obtained (~900 cP in this case from a 4.1 wt% solution of $1x10^6$ g/mol PEO), the pretreated hectorite was added, stirred and sonicated to obtain uniform suspensions. Concentrations of hectorite ranging from 0.5 to 30% (w/w) were dispersed in the aqueous PEO solutions. Uniform dispersions could be obtained at low concentrations (0.5% w/w) by stirring (~24 h) and sonication (five 30 minute durations using Branson 2200 bath sonicator). However, as the concentration of the hectorite was increased, extended periods of stirring (2-3 days) and sonication (eight to ten 30 minute durations) in between were necessary to form uniform dispersions. Homogenous PEO-hectorite dispersions, with hectorite concentrations of 0.5, 5, 10 and 20% were successfully prepared using the 10^6 g/mol molecular weight of PEO. Homogenous dispersion of clay could not be obtained with clay concentrations ≥ 30 wt%. The use of very high molecular weights of PEO (≥ $5x10^6$ g/mol), led to phase separation between hectorite and PEO. Uniform dispersions of hectorite clay with concentrations ≥ 10 wt% could not be obtained with low ($2x10^6$ g/mol) molecular weight PEO. Hence, unless otherwise noted all subsequent experiments were performed using 10^6 g/mol molecular weight PEO.

Once a visually homogenous suspension of PEO and clay was formed it was transferred to the 3 mL plastic syringe barrel, which was connected to nitrogen gas driven fluid dispensing system (EFD 1500 XL). A positive nitrogen pressure (~7 psi) was applied to maintain a droplet of the viscous gel at the needle tip. A DC voltage of 20

kV was applied using a Sorensen H. V. Supply (model # 1020-30) which, initiates the polymer/clay jet. The composite fibers forming in the jet were collected onto an aluminum foil target positioned 23 cm from the needle tip.

The viscosities of the solutions used were measured using a spindle and cone type Brook Field viscometer rotating the sample at 0.5 rpm. The size and morphology of the fibers were determined by scanning electron microscope using Philips XL30 scanning electron microscope (SEM) and the interaction of the polymer with the clay material was analyzed with a JOEL 1230 transmission electron microscope (TEM). Thin sections of fiber mesh embedded in epoxy were used for TEM analysis. X-ray diffraction (XRD) patterns were obtained using Scintag 2000 XDS diffractometer using a Cu Kα radiation. Infrared spectra were obtained using a Nicolet Avatar 360 spectrophotometer (resolution of 4 cm^{-1} and 100 scans per spectrum) on fibers that were directly electrospun onto KBr pellets. Thermal properties were analyzed using a Pyris Series-Diamond differential scanning calorimeter (DSC), on samples sealed in aluminum pans. The samples were heated from 20 °C to 100 °C and cooled back from 100 to 20 °C at the rate of 5°C/ minute to determine the melting and crystallization temperatures. Each cycle of heating and cooling was repeated three times to minimize artifacts due to preparation history. Properties of PEO/hectorite composites were compared to the bulk PEO and pure PEO electrospun fibers where ever possible.

3. RESULTS AND DISCUSSION

SEM images of a mesh of electrospun PEO fibers deposited for ~5 minutes (Figure 2) show that PEO can be spun into a dense network of fibers which are in the order of 100-200 nm, similar to previous reports [16-20]. PEO ($9x10^5$ g/mol MW) fibers have been spun from solutions with viscosities as low as 74 cP to as high as 1845 cP, with the fiber uniformity improving with increasing viscosity [16]. After 5 minute depositions we observe a mesh ~4-5 mm thick.

The non-uniform dispersions observed for very high MW ($5x10^6$ g/mol) of PEO is most likely due to reduced polymer mobility which in turn impeded clay intercalation. Increased particle-particle bridging is known to increase with molecular weight leading to a decrease in inter-particle collisions, a well known phenomenon called flocculation in colloids [24-26].

3.1 Microscopy

Figure 3 shows the SEM images of several PEO-hectorite composites with an increasing amount of clay (5, 10, 20 and 30% w/w). The morphology of the composite fibers differs from the pure PEO fibers where the composite fibers appear rough and may represent some aggregation of clay. The average diameter of the fibers is about 200 nm for composites containing up to 20% clay. However, with the 30% w/w clay composite, the fiber sizes increased to ~400-500 nm. The average thickness of the 10% w/w clay composite fiber mesh was 5-6 μm after 4-5 minute deposition time. As the amount of clay increased, the thickness of the mesh decreased, (figure 4) probably because of clay occupying more space in the composites. When electrospun, PEO solutions (10^6 g/mol MW) (viscosity

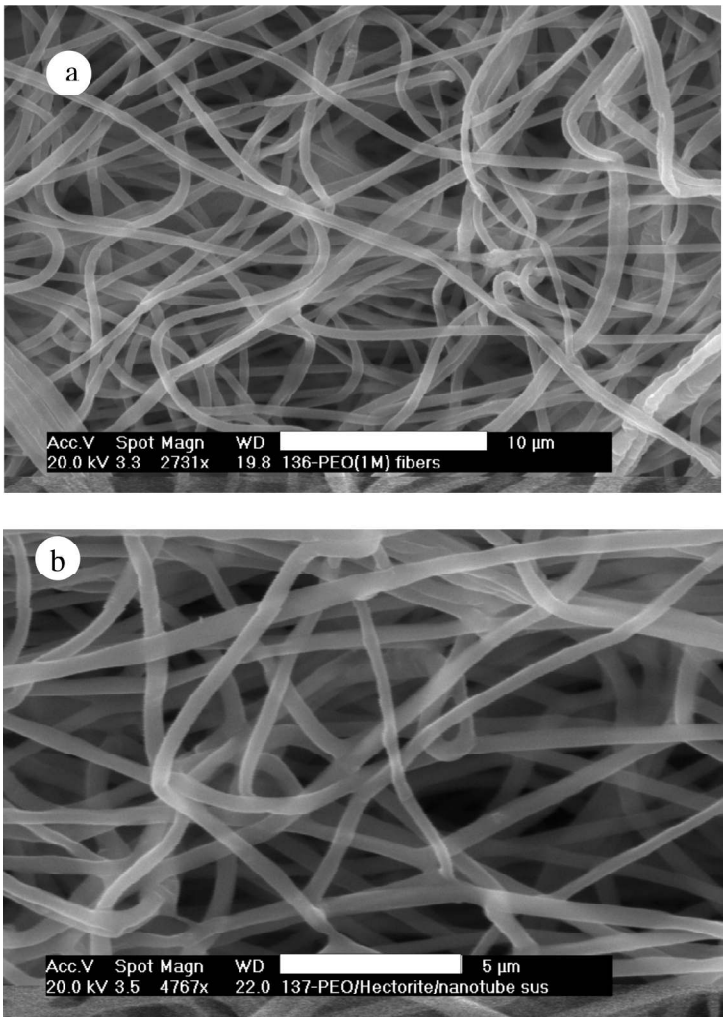

Figure 2: (a) and (b) 10^6 g/mol MW PEO electrospun fibers after ~5 minute deposition.

~9000 cp) formed webs which were localized around the electrode. However, uniform distribution of the fibers and the web was observed for the PEO/hectorite composite probably because of the charge associated with the clay particles. The TEM image of a thin cross-section of the fiber mesh shown in figure 5 suggests that there is intimate mixing and good interaction between the polymer and the clay material. Further more the layers of the clay material which are about 2 nm in thick which an interlayer spacing of 18 Å are intact as can be clearly seen in the places marked. Hence the polymer mainly intercalates between the layers of the clay but does not exfoliate it. This is in contrast with the totally exfoliated layers of organo layered silicate dispersed in polystyrene [11]. X-ray diffraction analysis (below) shows the interlayer d-spacing of the clay material increases by the intercalation of the polymer.

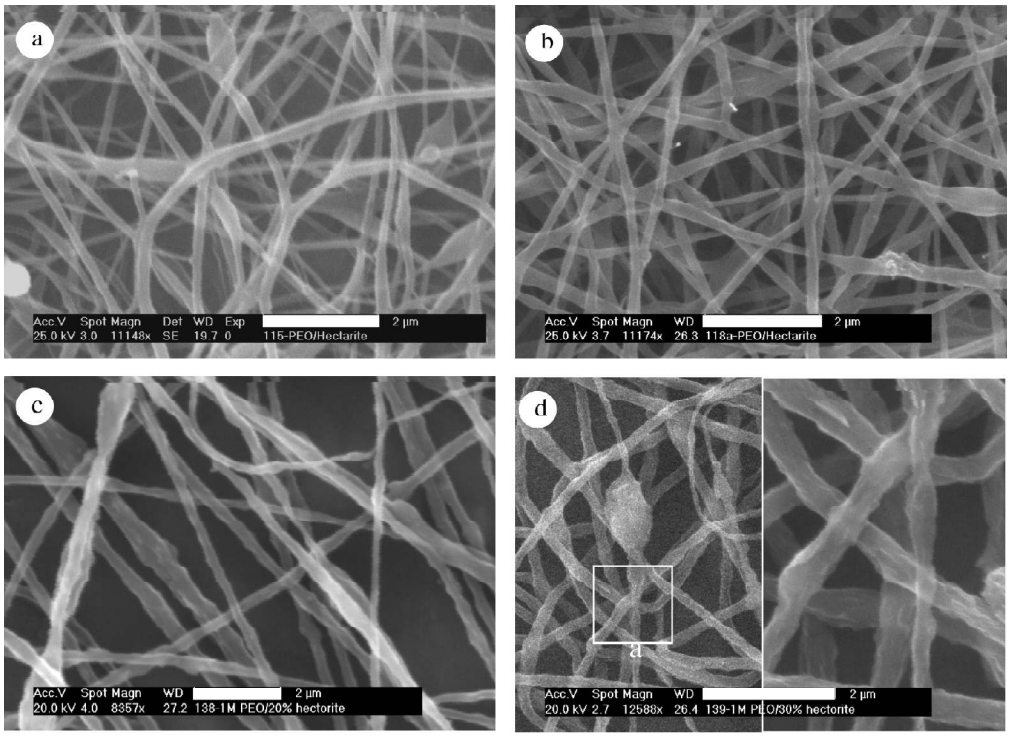

Figure 3: Scanning electron micrographs of PEO/hectorite composite fibers obtained with ~5 minute deposition times a) 5% hectorite b) 10% hectorite c) 20% hectorite and d) 30% hectorite (a region of the sample shown in the box zoomed in, the 2 mm scale bar corresponds to the zoomed in portion).

3.2 X-ray Diffraction

The powder x-ray diffraction patterns for bulk hectorite, bulk PEO, PEO fibers and PEO/30% hectorite composite fibers are shown in figure 6. Although the structure of aluminosilicates is sensitive to acidic environments, the x-ray diffraction pattern for the purified bulk material (figure 6b) shows that the structural integrity was maintained after the cleaning process. The x-ray patterns (not shown) obtained for 10 and 20% hectorite/PEO composites were similar but comparatively weaker because of the lower clay loading. The X-ray patterns of PEO/30% hectorite composite fibers and bulk hectorite (figures 6a and 6b), show that the 00*l* d-spacing of the hectorite has increased by about 6 Å in the composite fibers (from 13.8 to 19.5 Å). This is consistent with intercalation of the PEO between the layers of hectorite, increasing the gallery height. An XRD pattern for bulk composite material of 30% hectorite suspended in PEO also showed a similar increase in d-spacing (figure 6c), which suggests that intercalation of PEO occurs in the precursor gel which increased the 00*l* d-spacing and that this increase is maintained in the fibers. We have also previously observed a 6 Å increase after the intercalation of PEO (10^6 g/mol MW) in 5 wt% gadolinium exchanged hectorite composites [6-7]. In the case

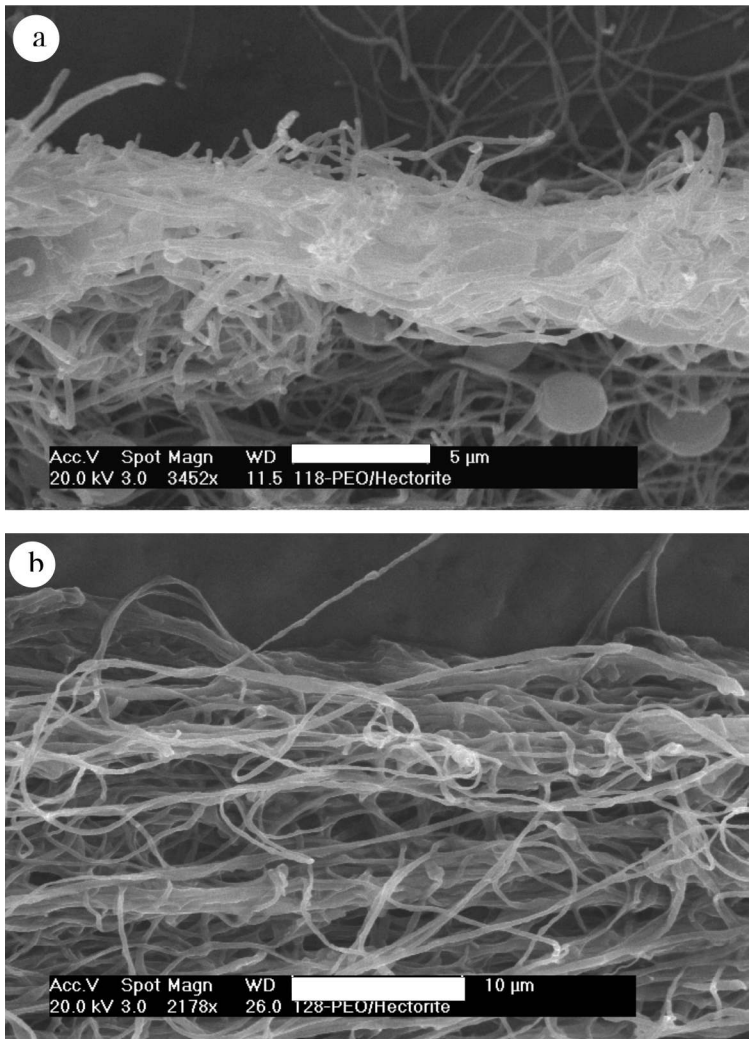

Figure 4: SEM image (at a 40° tilt) of the mesh obtained with electrospun fibers (a) PEO/ 10% hectorite, and (b) PEO/20% hectorite.

of related montmorillonite clays, the intercalation of PEO (10^5 g/mol MW) was found to expand the interlayer spacing by 6 - 8 Å. [8-9] Exfoliation of montmorillonite clay was reported in nylon 6-montmorillonite electrospun fibers (not quantified) [13].Therefore, it is reasonable to conclude that PEO is intercalated in the electrospun PEO/clay composite fibers as reported here.

Comparing the XRD patterns of bulk PEO and PEO electrospun fibers (Figures 6d and 6e) it is clear that, the crystallinity of PEO fibers has decreased. Considering the way the fibers are formed under the influence of electric field, the rapid solvent evaporation might lead to a different packing of the polymer molecules, and a kinetic trapping of

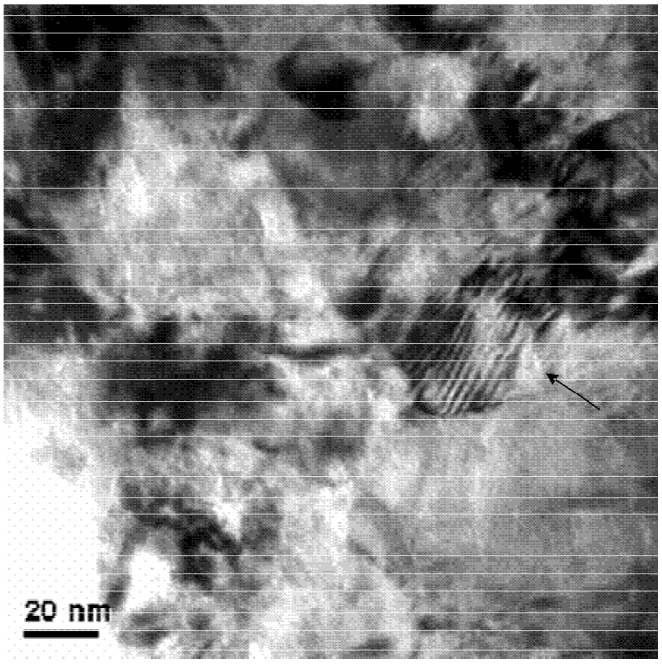

Figure 5: TEM image of an electrospun fiber mesh of PEO/10% hectorite composite fibers (in tact clay particles displaying 18 Å interlayer spacing are shown by the arrows).

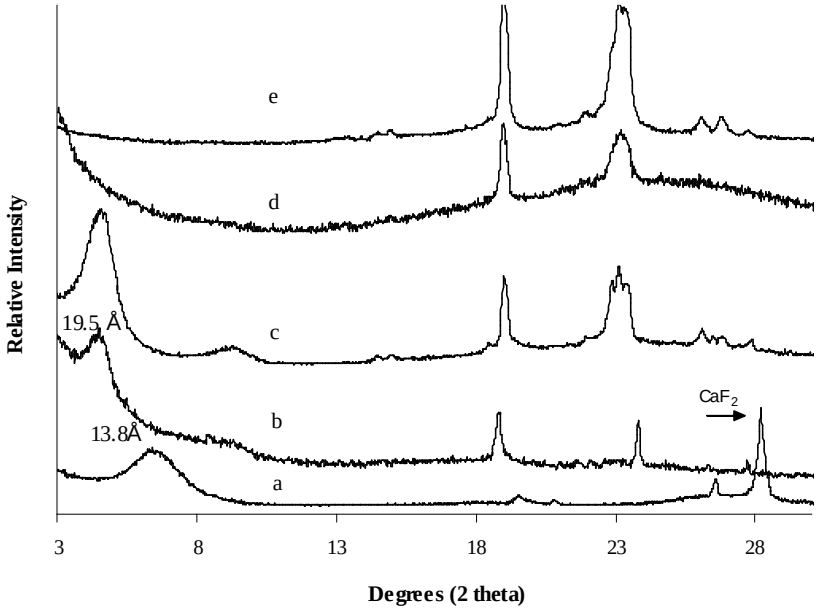

Figure 6: XRD patterns of (a) bulk hectorite, (b) electrospun PEO/30%hectorite composite fibers, (c) PEO/10% hectorite bulk composite (d) electrospun PEO fibers and (e) bulk PEO.

some amorphous component which leads to a decrease in crystallinity. Such a decrease in the crystallinity of PEO ($4x10^5$ g/mol MW) fibers compared to the bulk, has also been reported by Deitzel *et al.* [17]. The two broad peaks for the PEO fibers, observed at 2q values of 19.0 and 23.3 degrees, which are also observed in our case, have been assigned to (120) and (112) reflections respectively [17]. Decrease in crystallinity was also reported for nylon 6 electrospun fibers when compared to solution cast films [13].

In the PEO 30% hectorite bulk composite (figure 6d), the peaks corresponding to PEO exactly overlap with the bulk PEO (figure 6e) indicating that the crystallinity of PEO is maintained in the bulk composite but decreases in the fibers. A broad feature observed in the XRD patterns of the composite samples (between 9-10° 2θ) which is absent in the pure samples is prominent in the bulk and fiber composites suggesting a change in the crystallinity of PEO in the composite. The two peaks observed at 2θ values of 19.0 and 23.8 for the composite fibers, are shifted from the corresponding peaks observed for the pure PEO fibers, and bulk PEO in this region suggesting the presence of a different crystal phase of PEO in the PEO/clay composite fibers.

3.3 Vibrational Spectroscopy

The FTIR spectra for bulk hectorite, bulk PEO, PEO and PEO/hectorite composite fibers electrospun directly on to a KBr pellet are shown in figure 7. The IR spectrum

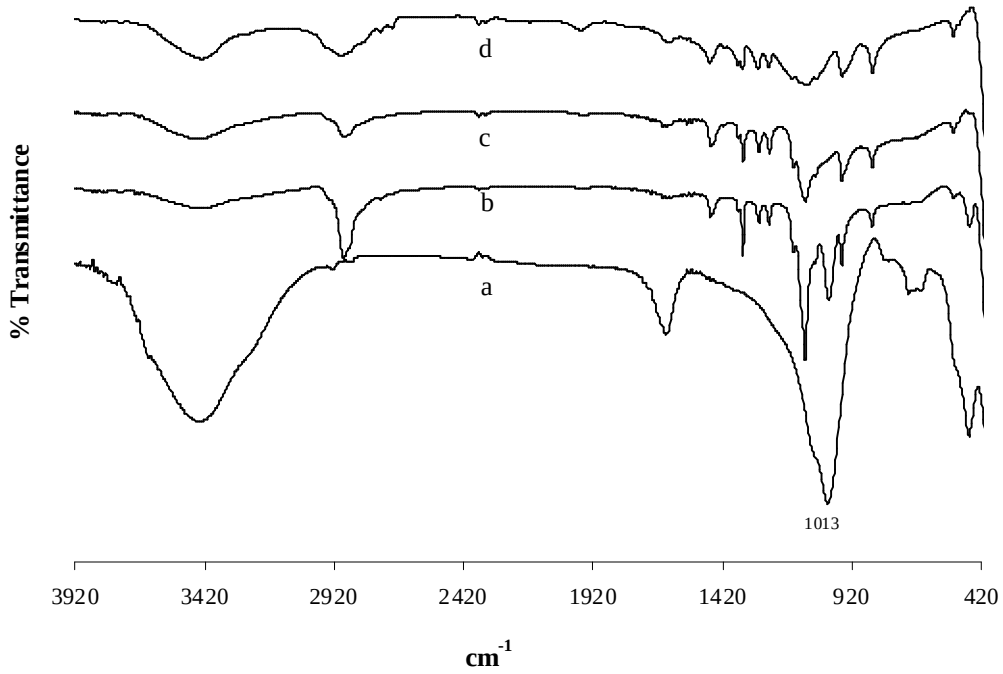

Figure 7: FT-IR spectra of (a) bulk hectorite, (b) electrospun PEO/20%hectorite composite fibers, (c) electrospun PEO fibers and (d) bulk PEO.

of the clay shown in figure 7a shows a broad Si-O asymmetric stretching band at 1013 cm^{-1} and another band at 474 cm^{-1}. The composite fibers show no significant shifts, which suggests that there are no structural changes to the clay (figure 7b). A comparison of the infrared spectra of bulk PEO (Figure 7d) and PEO fibers (figure 7c), reveals slight shifts towards lower wave numbers in the FTIR spectrum of fibers for bands in the conformation sensitive region (1500–1000 cm^{-1}) [8]. The band at 1477 cm^{-1}, which corresponds to -CH_2 scissoring mode is shifted to 1469 cm^{1}. The band at 1346 cm^{-1} corresponding to –CH_2 wag is shifted to 1342 cm^{-1}. The peaks at 1288 and 1245 cm^{-1} corresponding to –CH_2 twist are shifted to 1280 and 1242 cm^{-1} respectively. This implies that there might be some conformational changes in the PEO chains when electrospun. The band at 1114 cm^{-1} that corresponds to the C-O stretch is shifted to 1106 cm^{-1} with slight sharpening. However, this band is not believed to be conformation dependent. The band at 964 cm^{-1} in the bulk is shifted to 960 cm^{-1} in PEO fibers and is assigned to –CH_2 rocking mode. The band at 844 cm^{-1} in the bulk and in the fibers, is assigned to C-O stretching and –CH_2 rocking modes. The peaks in the 2890 cm^{-1} region in both the samples are assigned to the C-H stretches. The PEO in the composite fiber samples appears spectroscopically similar to the PEO fiber sample and is also shifted. The IR spectra of the composite fibers not only demonstrate the presence of both the materials, but also show some shifts in the polymer and clay components consistent with intercalation. Shifts in FT-IR spectra, to lower frequencies have been reported for PEO/ $Li_2CF_3SO_3^+$/Na montmorillonite composite systems.

3.4 Thermal Analysis

Thermal properties of the polymer and the polymer/clay composites were evaluated by DSC. Since the x-ray diffraction data of the PEO and the PEO/hectorite composite samples indicate changes in PEO crystallinity and give evidence of intercalation, changes in the melting point and the crystallization temperature were expected. Figure 8 shows the DSC data obtained for bulk PEO, PEO fibers and the electrospun composite fibers containing 10% and 30% hectorite. Comparing figures 8a and 8b we note that the melting point of PEO decreases from 62.5 °C in the bulk polymer to 59.1 °C in the electrospun fiber sample. This might be due to change in crystallinity in the fibers, which is also consistent with the presence of fewer reflections in the XRD patterns compared to bulk. This also translates into different crystallization temperatures for the bulk (43.7 °C) and for the fibers (40.2 °C). The polymer and the fibers were held at 100 °C for 10 minutes before cooling. Three cycles were recorded to ensure that these changes are not artifacts. There was a change in the melting and crystallization temperatures observed between the first and subsequent two heating and cooling cycles (DSC data for the first cycles shown as figure 1 in supplemental info). The data obtained from the third cycle were taken into consideration for further analysis. Change in crystallization temperatures between the first and second heating cycles were reported for poly-L-lactic acid (PLLA) which were attributed to possible rapid structure formation during the process of electrospinning [15]. However, melting and crystallization temperatures for the bulk PLLA were not reported. Also, crystallinity of electrospun PLLA fibers was reported to be lower (35-40%) than the ones obtained from melt (60%) and dilute solutions (90%).

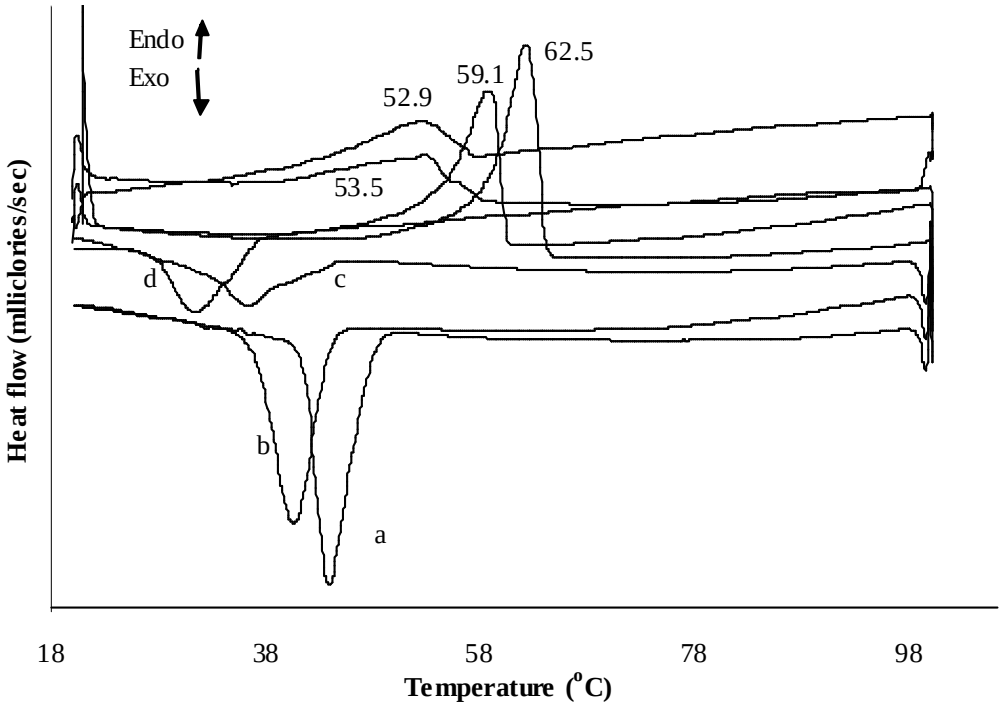

Figure 8: Endotherms showing change in melting points of (a) bulk PEO (b) electrospun PEO fibers (c) electrospun PEO/10%hectorite composite fibers, and (d) electrospun PEO/30%hectorite composite fibers

Comparing the endotherms of PEO fibers and PEO/10% hectorite composite fibers (figure 8b and 8c), there is a decrease in the melting point of PEO in the composite sample to 52.9 °C. Also, the peak for the composite sample is broader and less resolved than those for the pure polymers. The presence of salts has been shown to decrease the melting point of PEO. For example, a decrease in the melting point of PEO ($4x10^6$ g/mol MW) from 67°C to 54.7 °C was reported for a PEO-KSCN (16/1) mixture [28]. Also, a decrease in melting point was observed with increasing concentration of KIO_3 in PEO ($6x10^6$ g/mol MW) (from 70 to 68.5°C for a 90/10 mixture and from 70 to 64.4 °C for a 70/30 mixture) [29]. The presence of cations in the clay, which may be interacting with the oxygen atoms of PEO, may contribute to the decrease in melting point of PEO in the composite. When the DSC trace obtained for PEO/10% hectorite composite was deconvoluted, three peaks were resolved (figure 2a in supplementary information). The most intense peak with a maximum at 52.9 °C corresponds to the melting point of the intercalated PEO and the one at 56.5 °C, probably corresponds to some unintercalated crystalline PEO strands in the composite. The reason for the appearance of an additional peak at 48.1 °C is not clear. When the DSC trace of PEO/30% hectorite composite (figure 8d) is compared with the PEO/10% hectorite composite (figure 8b), a further

decrease in melting point (from 52.9 to 52.5 °C) is observed with a similar weak, broad peak in the temperature range of 55-59 °C. In addition, the presence of clay in the composites may cause the polymer to form smaller crystallites which in turn decrease the melting point. When this DSC trace was deconvoluted, two peaks one with a peak maximum at 52.5 °C (corresponding to the melting point of the intercalated PEO) and another with a peak maximum of 47.1 °C appear (figure 2b in supplementary information). However, the peak with a maximum at ~56 °C corresponding to unintercalated PEO was not found. As the concentration of hectorite is increased, the unintercalated PEO content is expected to decrease in the composite. The presence of a broad feature in the temperature range of 55-59 °C in the raw DSC trace (figure 8d) does suggest that there might be some unintercalated PEO present in the PEO/30% hectorite composite. However, the concentration of the unintercalated PEO might be less than that in the PEO/10% hectorite composite which might have led to the complete absence of the peak in the deconvoluted plots. Also, further decrease in crystallization temperature (30.8 °C) of PEO in PEO/30% hectorite composites was also observed. This is consistent with the presence of more charged particles as we increase the amount of clay [29]. A decrease in melting point from ~70 to ~63 °C have been reported for PEO ($1.9x10^4$ g/mol MW)-silica composites [30] and from ~62 to 55 °C in partially intercalated PEO (10^5 g/mol MW)/Na-montmorillonite composites [9]. However, the melting point change depends on the composite matrix PEO is in. For example, in an organic network with 30 wt% trimethopropane trimethacrylate, the melting point of PEO ($1.9x10^4$ g/mol MW) decreased from ~70 to ~52 °C [31]. The thermal analysis clearly shows that the crystallinity of PEO in the form of electrospun fibers in pure and composite forms is different from the bulk probably due to different crystallites and different sizes of the fibers formed in the absence and in the presence of clay respectively.

4. CONCLUSION

In conclusion, we have demonstrated that PEO can be intercalated in between the layers of hectorite clay and the resulting composite can be electrospun into nanofibers. The fibers have been characterized and the change in the properties of the composite sample compared to bulk is attributed to intercalation of PEO between the layers of hectorite. Once this can be shown, this concept can be extended to form nanofibers of composites with other interesting systems which have a wide variety of applications.

5. ACKNOWLEDGEMENTS

We sincerely thank Robert Welch Foundation for the financial support provided for this research and Aimei Wu for providing the TEM analysis on the composite samples.

References

[1] Y. Kojima, A. Usuki, M. Kawasumi, O. Okada, Y. Fukushima, T. Kurachi and O. Kamigaito, Mechanical Properties of nylon 6-clay hybrid, J. Mater. Res. 8 (1993) 1185-1189.

[2] Y. Ke, C. Long, and Z. Qi, Crystallization, Properties, and Crystal and Nanoscale Morphology of PET-clay Nanocomposites, J. Appl. Polym. Sci. 71 (1999) 1139-1146.

[3] G. Schmidt, A. I. Nakatami, P. D. Butler, V. Ferreiro, A. Karim, and C. Charles, Polymer-clay Nanocomposite Materials: Solution and Bulk Properties, Mater. Res. Soc. Symp. Proc. 661 (2001) KK5.10/1.

[4] P. W. Faguy, W. Ma, A. J. Lowe, and T. J. Brown, Conducting Polymer–clay Composites for Electrochemical Applications, J. Mater. Chem. 4 (1994) 771-772.

[5] T. W. Lee, O. O. Park, J. Yoon, and J. J. Kim, Enhanced Quantum Efficiency in Polymer/layered Silicate Nanocomposite light-emitting Devices, Syn. Met. 121 (2001) 1737-1738.

[6] K. J. Balkus, Jr., and J. Shi, A Study of Suspending Agents for Gadolinium (III)-Exchanged Hectorite. An Oral Magnetic Resonance Imaging Contrast Agent, Langmuir 12 (1996) 6277-6281.

[7] K. J. Balkus, Jr., and J. Shi, Studies of Gadolinium(III)-Modified Hectorite Clays as Potential Oral MRI Contrast Agents, J. Phys. Chem. 100 (1996) 16429-16434.

[8] J. Bujdak, E. Hackett and E. P. Giannelis, Effect of Layer Charge on the Intercalation of Poly(ethylene oxide) in Layered Silicates: Implications on Nanocomposite Polymer Electrolytes, Chem. Mater. 12 (2000) 2168.

[9] R. A. Vaia, S. Vasudevan, W. Krawiec, L. G. Scanlon and E. P. Giannelis, New Polymer Electrolyte Nanocomposites: Melt Intercalation of Poly(ethylene oxide) in mica-type silicate, Adv. Mater. 7 (1995) 154-156.

[10] M. Holtz, T. R. Park, J. Amarasekera, S. A. Solin, and T. J. Pinnavaia, The Influence of Guest–Host Interactions on the Guest Molecule in Intercalated Alumino-silicate Compounds, J. Chem. Phys. 100 (1994) 3346.

[11] R. Krishnamoorthi, R. Vaia, and E. P. Giannelis, Structure and Dynamics of Polymer-Layered Silicate Nanocomposites, Chem. Mater. 8 (1996) 1728.

[12] L. Ruban, S. Lomakin, and J. Zaikov, J. Polymeric Mater. 47 (2000) 117.

[13] H. Fong, W. Liu, C. Wang, and R. A. Vaia, Generation of Electrospun Fibers of nylon 6 and nylon 6-montmorillonite Nanocomposite, Polymer 43 (2002) 775.

[14] A. G. MacDiarmid, W. E. Jones, Jr., J. Gao, A. T. Johnson, Jr., N. J. Pinto, J. Hone, B. Han, F. K. Ko, H. Okuzaki and M. Llaguno, Electrostatically-generated Nanofibers of Electronic Polymers, Syn. Met. 119 (2001) 27.

[15] M. Bognitzki, W. Czado, T. Frese, A. Schaper, M. Hellwig, M. Steinhart, A. Greiner, and J. H. Wendroff, Nanostructured Fibers via Electrospinning, Adv. Mater. 13 (2001) 70-72.

[16] H. Fong, I. Chun, and D. H. Reneker, Beaded Nanofibers Formed during Electrospinning, Polymer, 40 (1999) 4585.

[17] J. M. Deitzel, J. Kleinmeyer, J. K. Hirvonen, and N. C. BeckTan, Polymer 42 (2001) 8163.

[18] J. Doshi, and D. H. Reneker, Electrospinning Process and Applications of Electrospun Fibers, J. Electrostat. 35 (1995) 151.

[19] Y. M. Shin, M. M. Hohman, M. P. Brenner, and G. C. Rutledge, Electrospinning: A Whipping Fluid Jet Generates Submicron Polymer Fibers, Appl. Phys. Lett. 78 (2001) 1149-1151.

[20] Yu-Quin Wan, Ji-Huan He, Jian-Yong Yu and Yue Wu, Electrospinning of High Molecule PEO Solution, J. Appl. Polym. Sci, 103 (2007) 3840-3843.

[21 D. J. Chaiko, New Poly(ethylene oxide)-Clay Composites, Chem. Mater., 15 (2003) 1105-1110.

[22] J. P. Lemmon, J. Wu, C. Oriakhi, and M. M. Lerner, Preparation of Nanocomposites Containing Poly(ethylene oxide) and Layered Solids, Electrochimica Acta, 40 (1995) 2245-2249.

[23] D. M. Moore, and R. C. Reynolds, Jr., in Structure and Properties of the Clay Minerals. *X-ray diffraction and the identification and analysis of clay minerals,* Oxford University Press: New York, 1989; pp102.

[24] T. G. M. Van De Ven, and B. J. Alince, Heteroflocculation by Asymmetric Polymer Bridging, J. Colloid. Interface. Sci., 181 (1996) 73-78.

[25] L.J. Burns, Y. Yan, J.G. Jameson and S. Biggs, The Effect of Molecular Weight of Nonadsorbing Polymer on the Structure of Depletion-Induced Flocs, J. Colloid. Interface. Sci. 247 (2002) 24-32.

[26] Y. Otsubo, Rheology of Colloidal Suspensions Flocculated by Reversible Bridging, Chem. Eng. Sci. 56 (2001) 2939-2946.

[27] H. W. Chen, and F. C. Chang, The Novel Polymer Electrolyte Nanocomposite Composed of Poly(ethylene oxide), Lithium Triflate and Mineral clay, Polymer, 42 (2001) 9763.

[28] W. Preechatiwong and J. M. Schultz, Electrical Conductivity of Poly(ethylene oxide)—Alkali Metal Salt Systems and Effects of Mixed Salts and Mixed Molecular Weights, Polymer, 37 (1996) 5109.

[29] J. M. Reddy, P. P. Chu, T. Sreenath, and S. U. V. Rao, Proton Conductor Based on poly(ethylene oxide) Complexed with tetra-methyl-ammonium bromide, Mater. Sci. Eng., B: Solid State Mater. Adv. Tech. 78 (2000) 59-62.

[30] S. Jiang, D. Yu, X. Ji, L. An, and B. Jiang, Confined Crystallization Behavior of PEO in Silica Networks, Polymer 41 (2000) 2041.

[31] S. Jiang, C. Qiao, S. Tian, X. Ji, L. An, and B. Jiang, Confined Crystallization behavior of PEO in Organic Networks, Polymer, 42 (2001) 5755.

Supplementary Information

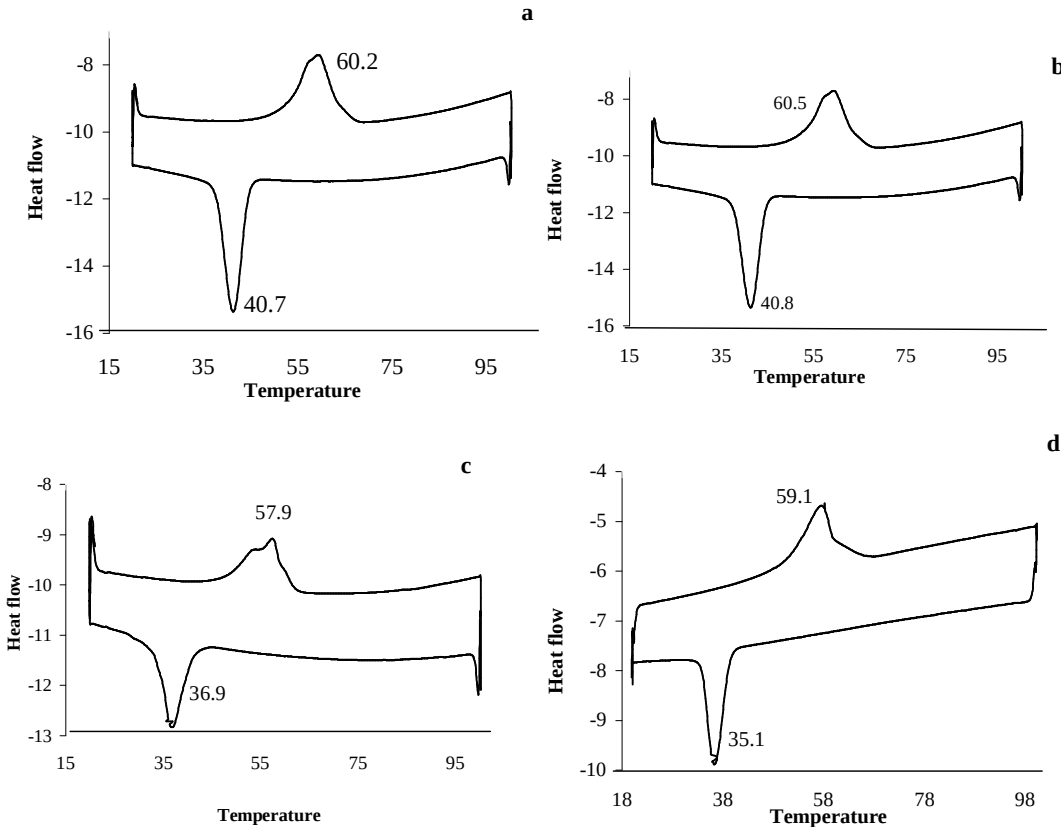

Figure 1: DSC scans obtained for the first heating-cooling cycle (a) Bulk PEO (10^6 g/mol MW), (b) Pure PEO fibers, (c) PEO/10% w/w hectorite composite fibers (d) PEO/ 30% w/w hectorite composite fibers.

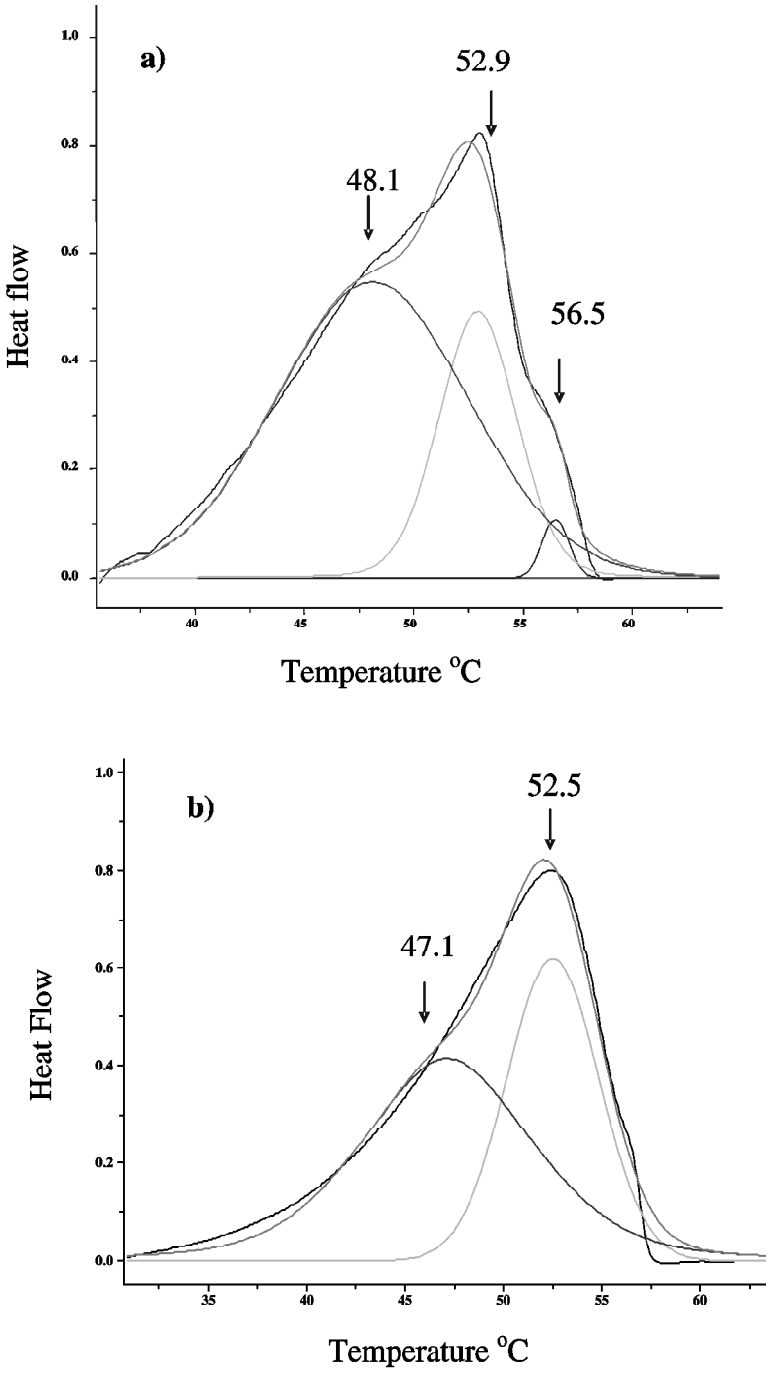

Figure 2: Deconvoluted DSC traces for the electrospun composite fibers (a) PEO/10% hectorite, (b) PEO/30% hectorite).